
Neural Time-Dependent Partial Differential Equation

Yihao Hu

University of Notre Dame
Notre Dame, IN 46556
yhu5@nd.edu

Tong Zhao

University of Notre Dame
Notre Dame, IN 46556
tzhao2@nd.edu

Zhiliang Xu

University of Notre Dame
Notre Dame, IN 46556
z xu2@nd.edu

Lizhen Lin

University of Notre Dame
Notre Dame, IN 46556
lizhen.lin@nd.edu

Abstract

Partial differential equations(PDEs) play a crucial role in studying a vast number of problems in science and engineering. Numerically solving nonlinear and/or high-dimensional PDEs is often a challenging task. Inspired by the traditional finite difference and finite element methods and emerging advancements in machine learning, we propose a sequence deep learning framework called Neural-PDE, which allows to automatically learn governing rules of any time-dependent PDE system from existing data by using a bidirectional LSTM encoder, and predict the next n time steps data. One critical feature of our proposed framework is that the Neural-PDE is able to simultaneously learn and simulate the multiscale variables. We test the Neural-PDE by a range of examples from one-dimensional PDEs to a high-dimensional and nonlinear complex fluids model. The results show that the Neural-PDE is capable of learning the initial conditions, boundary conditions and differential operators without the knowledge of the specific form of a PDE system. In our experiments the Neural-PDE can efficiently extract the dynamics within 20 epochs training, and produces accurate predictions. Furthermore, unlike the traditional machine learning approaches in learning PDE such as CNN and MLP which require vast parameters for model precision, Neural-PDE shares parameters across all time steps, thus considerably reduces the computational complexity and leads to a fast learning algorithm.

1 Introduction

The research of time-dependent partial differential equations (PDEs) is regarded as one of the most important disciplines in applied mathematics. PDEs appear ubiquitously in a broad spectrum of fields including physics, biology, chemistry, material science and finance, just to name a few. Despite their fundamental importance, most PDEs can not be solved analytically and have to rely on numerical solving. Developing efficient and accurate numerical schemes for solving PDEs, therefore has been an active research area over the past a few decades [1–6]. Still, devising stable and accurate schemes with acceptable computational cost is a difficult task especially when nonlinear and(or) high-dimensional PDEs are considered. Additionally, PDE models emerged from science and engineering applications usually require vast empirical data for model calibration and validation, and determining the multi-dimensional parameters in such a PDE system poses another challenge [7].

Deep learning is considered to be the state-of-the-art tool in classification and prediction of nonlinear inputs such as image, text, and speech [8–12]. Recently, tremendous efforts have been made to employ deep learning tools in designing data-driven methods for solving PDEs [13–16]. Most approaches

above are based on fully-connected neural network (FCNNs), convolutional neural network (CNNs) and multilayer perceptron (MLP), such structures usually require the increment of the layers to improve the predictive accuracy [16], and will also lead to a more complicated model due to the additional parameters. Recurrent Neural Networks (RNNs) is one type of neural network architectures which predict the next time step value by using the input data from the current and previous states, and share parameters across all inputs. This idea of using current and previous step solutions to calculate the solution at the next time step is not unique to RNNs. In fact, it is ubiquitously used in numerical PDEs. Almost all time-stepping numerical methods applied to solving time-dependent PDEs, including Forward Euler, Crank-Nicolson, high-order Taylor and its variance Runge-Kutta [17] time-stepping methods update numerical solution by utilizing solution from previous steps.

Motivated by the similarities between numerical methods of PDEs and recurrent neural network structure, we propose a new data-driven framework for solving system of PDEs. In this paper, the following two important questions are exploited:

- Is RNN or LSTM (Long Short-Term Memory) an efficient data-driven network to learn the solutions of time-dependent PDEs from prior data?
- Can machine learning be used to learn the governing physical laws directly from data without deriving the PDEs?

RNNs and similar types of artificial neural network update the current state output based on its previous time step value and current input [18]. This motivates us to think what would happen if we replace the previous time step data in the neural network with PDE solution data supported on grids. It is possible that the neural network behaves like a time-stepping method, for example, forward Euler method to yield the numerical solution at a new time point as the current state output [19]. Since the numerical solution on each of the grid point (for finite difference) or grid cell (for finite element) at a set of contiguous time points can be treated as input of one time sequence of data, the deep learning framework can be trained to learn from the time series data on all related mesh grid if the bidirectional structure is applied [20, 21]. In other words, the supervised training process can be regarded as a practice of the deep learning framework to learn the numerical method from the input data, by learning the coefficients of all related mesh grid data. For detailed methodology and mathematical proofs, please see Section 3.1 of the paper.

Long Short-Term Memory (LSTM) [22] is an advanced sequence model that is built upon RNNs. Unlike vanilla RNNs, which suffers from losing long term information and high probability of gradient vanishing or exploding, LSTM has a specifically designed memory cell with a set of new gates such as input gate and forget gate. Equipped with these new gates which control the time to preserve and pass the information, LSTM is capable of learning long term dependencies without danger of having gradient vanishing or exploding. In the past two decades, LSTM has been widely used in the field of natural language processing (NLP) such as machine translation, dialogue systems, question answering systems [23].

Inspired by numerical PDE schemes and LSTM neural network, we proposed a new deep learning framework, denoted as Neural-PDE, to learn multi-dimensional governing laws of any time-dependent PDE from the time series data of its mesh grids and predict the next n time steps data. The Neural-PDE is capable of intelligently processing related data from all spatial mesh grids by using the bidirectional [21] neural network, thus guarantees the accuracy of the numerical solution and the feasibility in learning high dimensional PDEs. The detailed structures of the model and data normalization are introduced in section 3.

In Section 4 of the paper we apply Neural-PDE to solve four different PDEs including the 1-dimensional (1D) wave equation, the 2-dimensional (2D) heat equation and two systems of PDEs: the inviscid Burgers' equations and a coupled Navier Stokes-Cahn Hilliard equations which widely appear in multiscale modeling of complex fluid systems. We demonstrate the robustness of Neural-PDE, which guarantees convergence within 20 epochs with an admissible mean square error even if we add Gaussian noise in the input data.

2 Preliminaries

2.1 Time Dependent Partial Differential Equations

A time-dependent partial differential equation is an equation of the form:

$$u_t = f(x_1, \dots, u, \frac{\partial u}{\partial x_1}, \dots, \frac{\partial u}{\partial x_n}, \frac{\partial^2 u}{\partial x_1 \partial x_1}, \dots, \frac{\partial^2 u}{\partial x_1 \partial x_n}, \dots, \frac{\partial^n u}{\partial x_1 \dots \partial x_n}), \quad (2.1.1)$$

where $u = u(t, x_1, \dots, x_n)$ is known, $x_i \in \mathbb{R}$ are spatial variables, and the operator f maps $\mathbb{R}^n \mapsto \mathbb{R}^m$. For example, the parabolic heat equation has the form: $u_t = \alpha^2 \Delta u$, where u represents the temperature, and f is the Laplacian operator: Δ . Eq. (2.1.1) can be solved by either finite difference or finite element methods which we briefly review below for the self-completeness of the paper.

2.2 Finite Difference Method

Consider to use a finite difference method (FDM) to solve a two-dimensional second order PDE of the form:

$$u_t = f(x, y, u_x, u_y, u_{xx}, u_{yy}), \quad (x, y) \in \Omega \subset \mathbb{R}^2, \quad t \in \mathbb{R}^+ \cup \{0\}. \quad (2.2.1)$$

Let Ω be $\Omega = [x_a, x_b] \times [y_a, y_b]$, and

$$u_{i,j}^n = u(x_i, y_j, t_n) \quad (2.2.2)$$

where $t_n = n\delta t$, $0 \leq n \leq N$, and $\delta t = \frac{T}{N}$ for $t \in [0, T]$. $x_i = i\delta x$, $0 \leq i \leq N_x$, $\delta x = \frac{x_a - x_b}{N_x + 1}$ for $x \in [x_a, x_b]$. $y_j = j\delta y$, $0 \leq j \leq N_y$, $\delta y = \frac{y_a - y_b}{N_y + 1}$ for $y \in [y_a, y_b]$.

The central difference methods indicates [5]:

$$u_x = \frac{1}{\delta x}(u_{i+1,j} - u_{i-1,j}) + \mathcal{O}(\delta x^2), \quad u_y = \frac{1}{\delta y}(u_{i,j+1} - u_{i,j-1}) + \mathcal{O}(\delta y^2) \quad (2.2.3)$$

$$u_{xx} = \frac{1}{\delta x^2}(u_{i+1,j} - 2u_{i,j} + u_{i-1,j}) + \mathcal{O}(\delta x^2), \quad u_{yy} = \frac{1}{\delta y^2}(u_{i,j+1} - 2u_{i,j} + u_{i,j-1}) + \mathcal{O}(\delta y^2) \quad (2.2.4)$$

Where $x_i = i\delta x$, $t(n) = n\delta t$. Therefore the explicit time-stepping to update next step solution u^{n+1} is given by:

$$u_{i,j}^{n+1} = u_{i,j}^n + \delta t f(x_i, y_j, u_{i,j}^n, u_{i,j-1}^n, u_{i,j+1}^n, u_{i+1,j}^n, u_{i-1,j}^n) + \mathcal{O}(\delta t^2, \delta x^2, \delta y^2) \quad (2.2.5)$$

$$= \mathbf{F}(x_i, y_j, \delta x_i, \delta y_j, u_{i,j}^n, u_{i,j-1}^n, u_{i,j+1}^n, u_{i+1,j}^n, u_{i-1,j}^n) + \mathcal{O}(\delta t^2, \delta x^2, \delta y^2) \quad (2.2.6)$$

2.3 Finite Element Method

Finite Element Method (FEM) is a powerful numerical method in solving PDEs. Consider a wave equation of $u(x, t)$:

$$u_{tt} - v^2 u_{xx} = f, \quad x \in \Omega \subset \mathbb{R}, \quad t \in \mathbb{R}^+ \cup \{0\}. \quad (2.3.1)$$

The function u is approximated by a function u_h :

$$u^n \approx u_h^n = \sum_i^N a_i^n \psi_i(x) \quad (2.3.2)$$

$$(2.3.3)$$

where $\psi_i \in V$, is the basis functions of some FEM space V , and a_i^n denotes the coefficients. N denotes the degrees of freedom.

Multiply the equation with an arbitrary test function ψ_j and integral over the whole domain we have:

$$\int_{\Omega} u_{tt} \psi_j dx + v^2 \int_{\Omega} \nabla u \nabla \psi_j dx = \int_{\Omega} f \psi_j dx \quad (2.3.4)$$

$$(2.3.5)$$

and approximate $u(x, t)$ by u_h :

$$\sum_i^N \frac{\partial^2 a_i^n}{\partial t^2} \underbrace{\int_{\Omega} \psi_i \psi_j dx}_{\mathbf{M}_{i,j}} + v^2 \sum_i^N a_i^n \underbrace{\int_{\Omega} \nabla \psi_i \nabla \psi_j dx}_{\mathbf{A}_{i,j}} = \underbrace{\int_{\Omega} f \psi_j dx}_{\mathbf{b}} \quad (2.3.6)$$

$$\equiv \mathbf{M}^T a_{tt}^n + v^2 \mathbf{A}^T a^n = \mathbf{b} \quad (2.3.7)$$

Here \mathbf{M} is the mass matrix and \mathbf{A} is the stiffness matrix, a^n is a $N \times 1$ vector of the coefficients at time $n\delta t$. The central difference method for time discretization indicates that[6]:

$$a^{n+1} = 2a^n - a^{n-1} + \mathbf{M}^{-1}(\mathbf{b} - v^2 \mathbf{A}^T a^n) \quad (2.3.8)$$

$$u^{n+1} \approx u_h^{n+1} = \sum_i^N a_i^{n+1} \psi_i(x) \quad (2.3.9)$$

Both numerical schemes (2.2.5) and (2.3.9) for updating u^{n+1} in finite difference and finite element method rely on the previous time step values of itself and its neighbourhoods. For instance, the central difference scheme will update u^{n+1} by using four points of u^n values. (see Figure 1), and the finite element method will approximate the new value by calculating the corresponded coefficients a^{n+1} , which is updated by its related nearby coefficients on the triangular mesh. (see Figure 2)

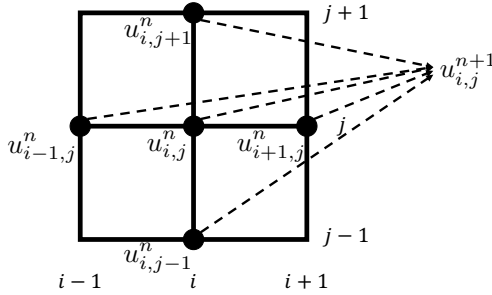


Figure 1: Update steps for a 2-dimensional central finite difference scheme

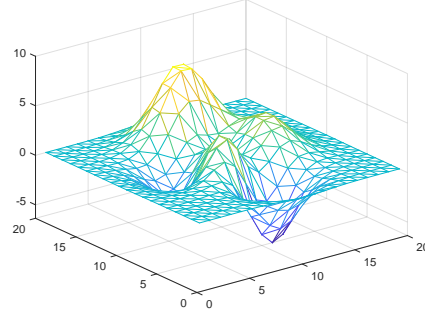


Figure 2: FEM triangular mesh for a 2-dimensional PDE

From another perspective, one may regard the updating schemes of numerical solutions of time dependent partial differential equations as catching the information from its neighbourhood data.

3 Proposed Method

3.1 Theoretical Motivation

Recurrent neural network including LSTM is an artificial neural network structure of the form [23]:

$$\mathbf{h}^t = \sigma(W^{hx} \mathbf{x}^t + W^{hh} \mathbf{h}^{t-1} + \mathbf{b}_h) \equiv f(\mathbf{x}^t, \mathbf{h}^{t-1}) \quad (3.1.1)$$

where \mathbf{x}^t is the input data of current state and \mathbf{h}^{t-1} denotes the processed value in its previous state by the hidden layers. The state output \mathbf{y}^t is updated by the current state value \mathbf{h}^t :

$$\mathbf{y}^t = \sigma(W^{hy} \mathbf{h}^t + \mathbf{b}_y) \quad (3.1.2)$$

Here W^{hx} , W^{hh} , W^{hy} are the matrix of weights and vectors \mathbf{b}_h and \mathbf{b}_y are the coefficients of bias, and here σ is the respected sigmoid function. With the design of input and forget gate, LSTM can effectively yield a better control over the gradient flow and better preserve useful information from long-range dependencies [24].

For a temporal continues \mathbf{h} , consider an ordinary differential equation with the form:

$$\frac{d\mathbf{h}(t)}{dt} = g(\mathbf{h}(t), \mathbf{x}(t), t) \quad (3.1.3)$$

In numerical analysis, a forward Euler method for $\mathbf{h} \in \mathbb{R}^n$ can be easily derived from the Taylor series and has the following approach:

$$\frac{\partial \mathbf{h}^t}{\partial t} = \frac{\mathbf{h}^t - \mathbf{h}^{t-1}}{\delta t} + \mathcal{O}(\delta t) \quad (3.1.4)$$

For the ODE case we may have:

$$\begin{aligned} \frac{d\mathbf{h}^t}{dt} = g(\mathbf{h}^{t-1}, \mathbf{x}^t, t) &\xrightarrow{(3.1.4)} \mathbf{h}^t = \mathbf{h}^{t-1} + \delta t g(\mathbf{h}^{t-1}, \mathbf{x}^t, t) + \mathcal{O}(\delta t) \\ &\rightarrow \mathbf{h}^t \equiv \mathbb{F}(\mathbf{h}^{t-1}, \mathbf{x}^t, t) \end{aligned} \quad (3.1.5)$$

Combining equations (3.1.1) and (3.1.5) one may notice that the residual networks, recurrent neural network and also LSTM networks can be regarded as a numerical scheme for solving differential equations if add more layers and take smaller time steps. [19].

Canonical structure for such recurrent neural network usually calculate the current state value by its previous time step value \mathbf{h}^{t-1} and current state input \mathbf{x}^t . Similarly, in numerical PDEs, the next value data is updated from the values on its nearby grid points (see Eq. 2.2.5).

Thus, what if we replace the temporal input \mathbf{h}^{t-1} and \mathbf{x}^t with spatial information? A simple sketch of Euler method for a 1D example of $u(x, t)$:

$$u_t + v u_x = 0 \quad (3.1.6)$$

will be:

$$u_i^{n+1} = u_i^n - v \frac{\delta t}{\delta x} (u_i^n - u_{i-1}^n) + \mathcal{O}(\delta x, \delta t) \equiv \mathbb{F}(\mathbf{x}_i, \mathbf{h}_{i-1}(u)) \quad (3.1.7)$$

$$\mathbf{x}_i = u_i^n \quad (3.1.8)$$

$$\mathbf{h}_{i-1}(u) = \mathbb{F}(u_0^n, u_1^n, \dots, u_{i-1}^n). \quad (3.1.9)$$

Here we replace the temporal previous state \mathbf{h}^{t-1} with spacial grid value \mathbf{h}_{i-1} and input u_i^n as current state value, which indicates the neural network could be seen as an forward Euler method for equation 3.1.6 [25]. By applying Bidirectional neural network, all mesh grid data is transferred and enables LSTM to simulate the higher order PDEs as :

$$u_i^{n+1} = \mathbb{F}(\mathbf{h}_{i+1}(u), u_i^n, \mathbf{h}_{i-1}(u)) \equiv 2.2.6 \quad (3.1.10)$$

$$\mathbf{h}_{i+1}(u) = \mathbb{F}(u_{i+1}^n, u_{i+2}^n, \dots, u_{N_x}^n). \quad (3.1.11)$$

For a time dependent PDE, if we map all our mesh grid data into input matrix which contains the information of $\delta x, \delta t$, then the neural network would regress such coefficients as constants and will learn and filter the physical rules from all the k mesh grids as:

$$u_i^{n+1} = \mathbb{F}(u_0^n, u_1^n, u_2^n, \dots, u_k^n) \quad (3.1.12)$$

The LSTM neural network is designed to overcome the vanishing gradient issue through hidden layers, therefore we use such recurrent structure to increase the stability of the numerical approach in deep learning. Similarly with the finite difference method (section 2.2) and finite element method (section 2.3), the highly nonlinear functional \mathbb{F} simulates the derivatives of u_i and thus ensure the feasibility of the Bidirectional LSTM encoder in the deep learning framework.

3.2 Long Short-Term Memory

Long Short-Term Memory Networks (LSTM) [22, 24] is a class of artificial recurrent neural network (RNN) architecture that is commonly used for processing sequence data and could overcome the gradient vanishing issue in RNN. Similar to most RNNs [26], LSTM takes a sequence $\{x_1, x_2, \dots, x_t\}$ as input and learns hidden vectors $\{h_1, h_2, \dots, h_t\}$ for each corresponding input. In order to better retain long distance information, LSTM cells are specifically designed to update the hidden vectors.

The computation process of the forward pass for each LSTM cell is defined as following:

$$\begin{aligned}
i_t &= \sigma(\mathbf{W}_i^{(x)}x_t + \mathbf{W}_i^{(h)}h_{t-1} + \mathbf{W}_i^{(c)}c_{t-1} + \mathbf{b}_i), \\
f_t &= \sigma(\mathbf{W}_f^{(x)}x_t + \mathbf{W}_f^{(h)}h_{t-1} + \mathbf{W}_f^{(c)}c_{t-1} + \mathbf{b}_f), \\
c_t &= f_t c_{t-1} + i_t \tanh(\mathbf{W}_c^{(x)}x_t + \mathbf{W}_c^{(h)}h_{t-1} + \mathbf{b}_c), \\
o_t &= \sigma(\mathbf{W}_o^{(x)}x_t + \mathbf{W}_o^{(h)}h_{t-1} + \mathbf{W}_o^{(c)}c_t + \mathbf{b}_o), \\
h_t &= o_t \tanh(c_t),
\end{aligned}$$

where σ is the logistic sigmoid function, \mathbf{W} are weight matrices, \mathbf{b} are bias vectors, and i, f, o and c are the input gate, forget gate, output gate and cell vectors respectively, all of which have the same size as hidden vector h .

In this work, we use the standard LSTM structure to simulate the numerical solutions of partial differential equations.

3.3 Neural-PDE

In this work, we take a neural sequence model that estimates PDE in the similar way as FDM and FEM does, that is, to inference the future state of a given point based on the past states of the points around it. We leverage the neural models well-known capability of serving as universal function approximators [27] to avoid calculating the actually numerical solutions of PDEs, which is extremely slow for large systems. Moreover, we proposed to use bidirectional LSTM [22, 24] to better retain the state information from far data points.

The right side of Figure 3 shows the overall design of Neural-PDE. Denoting the time series data at collocation points as u_1, u_2, \dots, u_n and with $u_i = [u_i^0, u_i^1, \dots, u_i^N]$. The model takes the past states of all points $\{u_1, u_2, \dots, u_n\}$ and outputs the predicted future states $\{p_1, p_2, \dots, p_n\}$, where $p_i = [u_i^{N+1}, u_i^{N+2}, \dots, u_i^{N+M}]$ is the model's future prediction for point u_i , where N is the time steps for training and M is the time steps for prediction.

Neural-PDE is an encoder-decoder style sequence model that first maps the input data to a low dimensional latent space that

$$h_i = \overrightarrow{\text{LSTM}}(u_i) \oplus \overleftarrow{\text{LSTM}}(u_i), \quad (3.3.1)$$

where \oplus is concatenation and h_i is the latent embedding of point u_i under the environment.

One then decode, another bi-lstm with a dense layer:

$$p_i = \left(\overrightarrow{\text{LSTM}}(h_i) \oplus \overleftarrow{\text{LSTM}}(h_i) \right) \cdot \mathbf{W}, \quad (3.3.2)$$

where \mathbf{W} is the learnable weight matrix in the dense layer.

During training process, mean square error (MSE) loss is used as we typically don't know the specific form of the PDE

$$\mathcal{L} = \sum_i ||u_i - p_i||^2, \quad (3.3.3)$$

where p_i is the predicted time series data on i^{th} grid point.

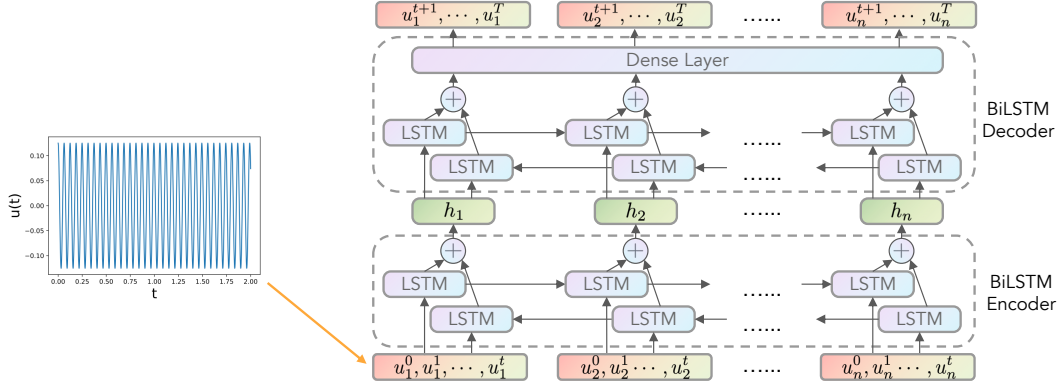


Figure 3: Neural-PDE

3.4 Data Initialization and Mesh Grid Reshape

In order to feed data into our sequence model framework, we map the PDE data into a $K \times N$ matrix, where $K \in \mathbb{Z}^+$ is the dimension of the grid points and $N \in \mathbb{Z}^+$ is the length of the time series data in each grid point. For example, a 2D heat equation at some time t will be reshaped into a 1D vector. (See Figure 4)

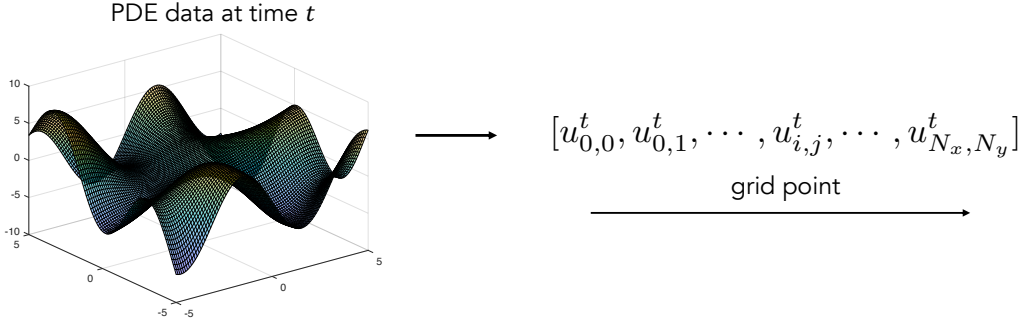


Figure 4: An example of mapping 2d data matrix into 1d vector where $N_x + 1$ and $N_y + 1$ are the number of grid points on x and y , respectively.

For a n dimensional time dependent partial differential equation with K mesh grid points, the input and output data for $t \in (0, T)$ will be of the form:

$$X_K^N = \begin{bmatrix} u_0 \\ u_1 \\ \vdots \\ u_K \end{bmatrix} = \begin{bmatrix} u_0^1 & u_0^2 & \cdots & u_0^n & \cdots & u_0^N \\ \vdots & \vdots & \ddots & \vdots & \ddots & \vdots \\ u_k^1 & u_k^2 & \cdots & u_k^n & \cdots & u_k^N \\ \vdots & \vdots & \ddots & \vdots & \ddots & \vdots \\ u_K^1 & u_K^2 & \cdots & u_K^n & \cdots & u_K^N \end{bmatrix} \quad (3.4.1)$$

$$Y_K^M = \begin{bmatrix} p_0 \\ p_1 \\ \vdots \\ p_K \end{bmatrix} = \begin{bmatrix} u_0^{N+1} & u_0^{N+2} & \cdots & u_0^{N+m} & \cdots & u_0^{N+M} \\ \vdots & \vdots & \ddots & \vdots & \ddots & \vdots \\ u_k^{N+1} & u_k^{N+2} & \cdots & u_k^{N+m} & \cdots & u_k^{N+M} \\ \vdots & \vdots & \ddots & \vdots & \ddots & \vdots \\ u_K^{N+1} & u_K^{N+2} & \cdots & u_K^{N+m} & \cdots & u_K^{N+M} \end{bmatrix} \quad (3.4.2)$$

Here $N = \frac{T}{\Delta t}$ and each row represents the time series at the corresponded mesh grid.

By adding Bidirectional LSTM encoder in Neural-PDE, the machine learning framework will automatically extract the information from its previous and following grid points:

$$Y_K^M = \mathbb{F}(X_K^N) = \mathbb{F}(u_0, u_1, \dots, u_i, \dots, u_K) \quad (3.4.3)$$

Here M is the time length of the predicted data. Thus ensure the Neural-PDE will automatically learn the time series data from itself and its neighbourhood regardless of the order of the grid points in the input matrix.

4 Experiments

Since Neural-PDE is a sequence to sequence learning framework which allows one to predict any time period by the given data. One may test different permutations of training and predicting time periods for the model optimization.

In the following experiments we will predict the next $t_p = 10 \times \delta t$ PDE solution by using its previous $t_{tr} = 30 \times \delta t$ data as:

$$Y_K^{10} = \mathbb{F}(X_K^{30}) \quad (4.0.1)$$

The whole dataset is randomly splitted in 80% for training and 20% for testing.

	1D Wave	2D Heat	2D Burgers	Multiscale
MSE	$7.4444E-5$	$7.0741E-6$	$1.4018E-5$	$6.1631E-7$
Parameters	0.09M	0.09M	0.09M	0.09M

Example 1: Wave Equation

Consider the 1D wave equation:

$$u_{tt} = cu_{xx}, \quad x \in [0, 1], \quad t \in [0, 2], \quad (4.0.2)$$

$$u(x, 0) = \sin(4\pi x) \quad (4.0.3)$$

$$u(0, t) = u(1, t) \quad (4.0.4)$$

Let $c = \frac{1}{16\pi^2}$ and use the analytical solution given by the characteristics for the training and testing data:

$$u(x, t) = \frac{1}{2}(\sin(4\pi x + t) + \sin(4\pi x - t)) \quad (4.0.5)$$

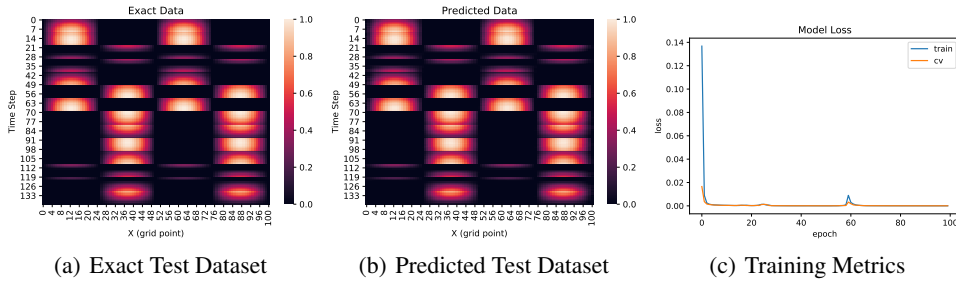


Figure 5: $\delta x = 1 \times 10^{-2}$, $\delta t = 1 \times 10^{-3}$, MSE: 7.4444×10^{-5} , the whole time period length is $n_t = 2000$ and the mesh grid size is 101, the test dataset size is 14 and thus the total discrete testing time period is 140, figure (a) and figure(b) are the heat map for the exact test data and our predicted test data. Figure(c) shows both training and cross-validation errors of Neural-PDE convergent within 10 epochs.

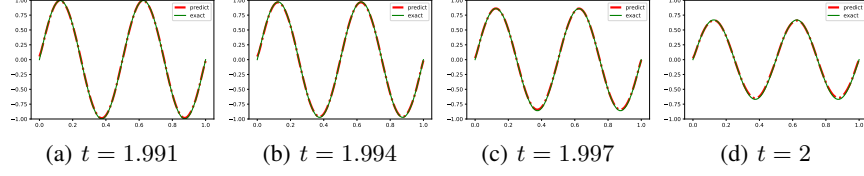


Figure 6: We selected the final states for computation and the results indicate that Neural-PDE is robust in capturing the physical laws of wave equation and predicting the sequence time period.

Example 2: Heat Equation

The heat equation describes how the motion or diffusion of a heat flow evolves over time. The Black–Scholes model [28] is also developed based on the physical laws behind the heat equation. Rather than the 1D case that maps the data into a matrix (3.4.1) with its original spatial locations, the high dimensional PDEs grids are mapped into matrix without regularization of the position, and the experimental results show that Neural-PDE is able to capture the valuable features regardless of the order of the mesh grids in the matrix. Let's start with a 2D heat equation as follows:

$$u_t = u_{xx} + u_{yy}, \quad (4.0.6)$$

$$u(x, y, 0) = \begin{cases} 0.9, & \text{if } (x - 1)^2 + (y - 1)^2 < 0.25 \\ 0.1, & \text{otherwise} \end{cases} \quad (4.0.7)$$

$$\Omega = [0, 2] \times [0, 2], \quad t \in [0, 0.15] \quad (4.0.8)$$

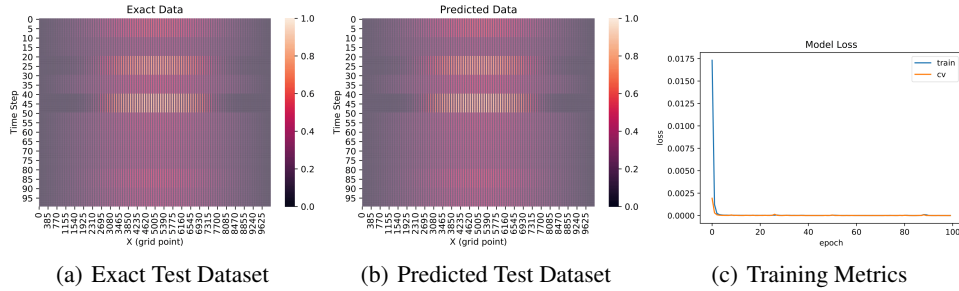


Figure 7: $\delta x = 0.02, \delta y = 0.02, \delta t = 10^{-4}$, MSE: 7.0741×10^{-6} , the size of the test data is 10 and the test time period is 140.

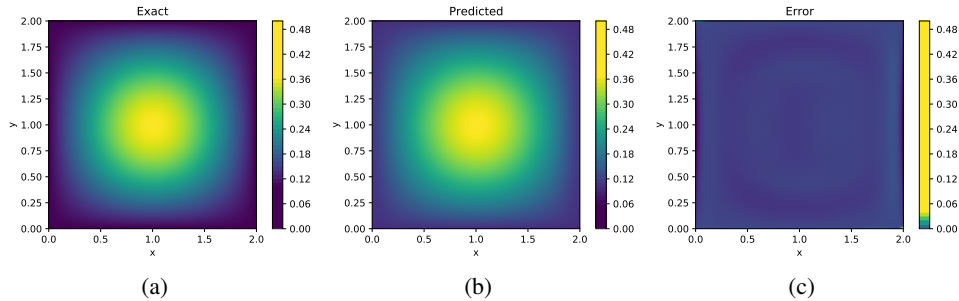


Figure 8: figure (a) is the exact solution $u(x, y, t = 0.15)$ at the final state and figure (b) is the model's prediction. Figure (c) is the error map.

Example 3: Inviscid Burgers Equation

The coupled inviscid burgers equation is a fundamental nonlinear PDE in fluid dynamics. The Burgers equation is derived from the famous Navier-Stokes equation by dropping the pressure term p . In this example, we will consider a inviscid burgers equation which has the following hyperbolic conservation form:

$$\frac{\partial u}{\partial t} + u \frac{\partial u}{\partial x} + v \frac{\partial u}{\partial y} = 0 \quad (4.0.9)$$

$$\frac{\partial v}{\partial t} + u \frac{\partial v}{\partial x} + v \frac{\partial v}{\partial y} = 0 \quad (4.0.10)$$

$$\Omega = [0, 1] \times [0, 1], t \in [0, 1], \quad (4.0.11)$$

and with Initial and Boundary conditions:

$$u(0.25 \leq x \leq 0.75, 0.25 \leq y \leq 0.75, t = 0) = 0.9 \quad (4.0.12)$$

$$v(0.25 \leq x \leq 0.75, 0.25 \leq y \leq 0.75, t = 0) = 0.5 \quad (4.0.13)$$

$$u(0, y, t) = u(1, y, t) = v(x, 0, t) = v(x, 1, t) = 0 \quad (4.0.14)$$

The inviscid Burgers equation is hard to deal with in classical numerical PDEs due to the discontinuities (shock waves), which is leaded by the zero part on the right hand side. We use a finite difference scheme to create the training data and couple the velocity u, v in to the input matrix. Our empirical results show that the Neural-PDE is able to learn the shock waves, boundary conditions and the rules of the fluid dynamics and predict u and v simultaneously.

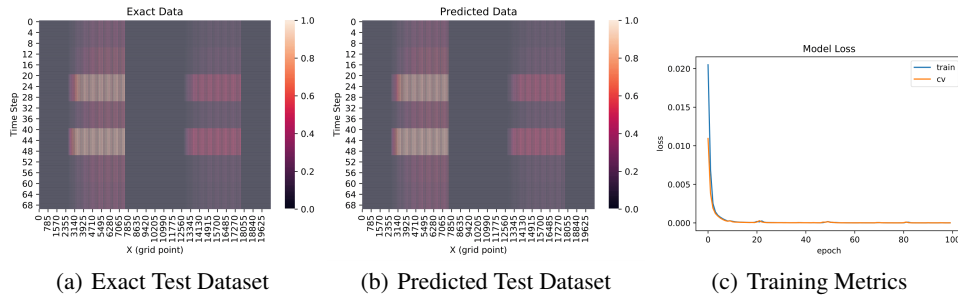


Figure 9: $\delta x = 1 \times 10^{-2}$, $\delta y = x = 1 \times 10^{-2}$, $\delta t = x = 1 \times 10^{-3}$, MSE: 1.4018×10^{-5} , the whole time series dataset has 31 batches and is splitted into 24 training data and 7 test data. The model loss still convergent within 20 epochs

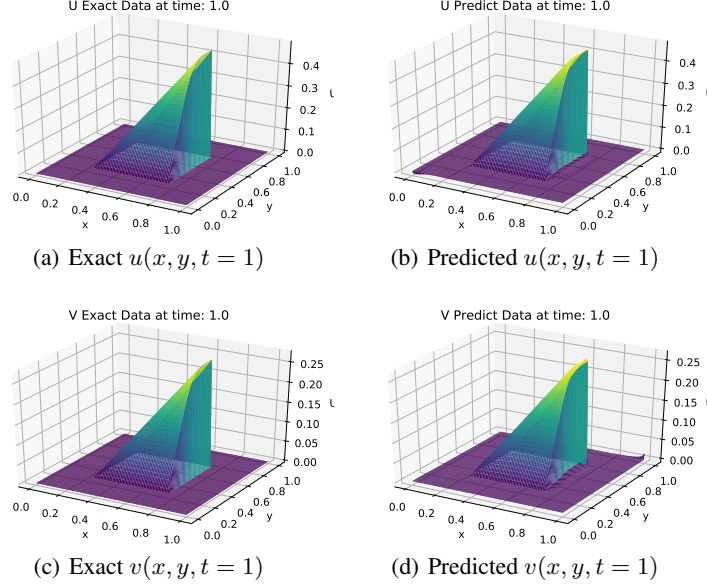


Figure 10: Exact and Prediction data of u and v at $t = 1$.

Example 4: Multiscale Modeling: Coupled Cahn–Hilliard–Navier–Stokes System

Finally, let's consider the following 2D Cahn–Hilliard–Navier–Stokes system widely used for modeling complex fluids:

$$u_t + u \cdot \nabla u = -\nabla p + \nu \Delta u - \phi \nabla \mu, \quad (4.0.15)$$

$$\phi_t + \nabla \cdot (u\phi) = M \Delta \mu, \quad (4.0.16)$$

$$\mu = \lambda(-\Delta \phi + \frac{\phi}{\eta^2}(\phi^2 - 1)) \quad (4.0.17)$$

$$\nabla \cdot u = 0 \quad (4.0.18)$$

In this complicated example we will use the following initial condition:

$$\phi(x, y, 0) = (\frac{1}{2} - 50 \tanh(f_1 - 0.1)) + (\frac{1}{2} - 50 \tanh(f_2 - 0.1)), \text{ I.C.} \quad (4.0.19)$$

$$f_1 = \sqrt{(x + 0.12)^2 + (y)^2}, \quad f_2 = \sqrt{(x - 0.12)^2 + (y)^2} \quad (4.0.20)$$

The coefficients are given as:

$$x \in [-0.5, 0.5], \quad y \in [-0.5, 0.5], \quad t \in [0, 1]$$

$$M = 0.1, \quad \nu = 0.01$$

This multiscale complex fluid system can be derived by the energetic variational approaches [29]. The complex fluids system has the following features: the micro-structures such as the molecular configurations, the interaction between different scales and the competition between multi-phase fluids [30]. Here u is the velocity and $\phi(x, y, t) \in [0, 1]$ denotes the volume fraction of one fluid phase. The system is consisted with one Navier-Stokes equation (4.0.15), a Cahn-Hilliard equation (4.0.16) [31], where M is the diffusion coefficient and μ is the chemical potential of ϕ , and equation (4.0.18) which indicates the incompressibility of the fluids. Solving such PDE system is notorious because of its high nonlinearity and multi-physical coupled features. One may use the decoupled projection method [32] to numerically solve it efficiently or use an implicit method which however is computationally expensive.

Another challenge of deep learning in multiscale modeling is how to process the data to improve the learning efficiency when the input matrix consists of large scale variable such as $\phi \in [0, 1]$ and infinitesimal values $p \sim 10^{-5}$. For Neural-PDE to better learn and extract the physical features

of variables in different scales, we normalized the p data with a *sigmoid* function and our model presents that the physical features of pressure and ϕ have been captured successfully.

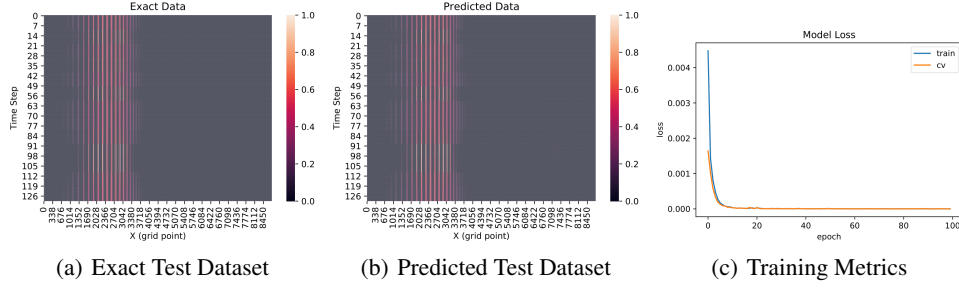


Figure 11: $\delta t = 5 \times 10^{-4}$, MSE: 6.1631×10^{-7} , the dataset is given by the FreeFem++[33] with a Crank-Nicolson based finite element scheme and has a batch size of 64.

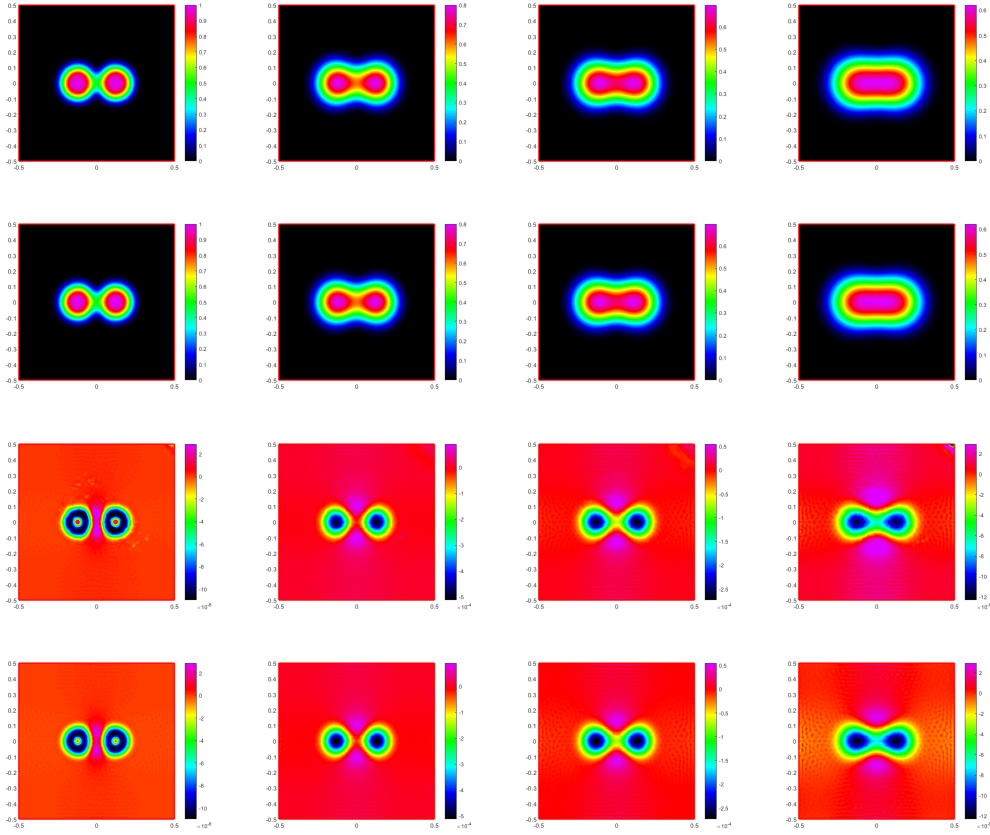


Figure 12: The first row is the predicted data and the second row is the exact data of ϕ , the third row is the plot of recovered prediction of pressure p and the fourth row is the exact plot of p . The graphs of each column from left to right represent the states of t_1, t_2, t_3, t_4 where $0 \leq t_1 < t_2 < t_3 < t_4 \leq 1$

5 Conclusions

In this paper, we proposed a novel sequence recurrent deep learning framework: Neural-PDE, which is capable of intelligently filtering and learning solutions of time-dependent PDEs. One key innovation of our method is that the collocation method from the numerical PDEs is applied in the

deep learning framework, and the neural network is trained to explore the accurate numerical methods for prediction.

Our experiments show that the Neural-PDE is capable of simulating from 1D to multi-dimensional scalar PDEs to highly nonlinear and coupled PDE systems with their initial conditions, boundary conditions without knowing the specific forms of the equations. Solutions to the PDEs can be either continuous or discontinuous.

The state-of-art researches have shown the promising power of deep learning in solving high-dimensional nonlinear problems in engineering, biology and finance with efficiency in computation and accuracy in prediction. However, there are still many crucial and unresolved issues in applying deep learning in PDEs. For instance, the stability and convergence of the numerical algorithms have been rigorously studied by applied mathematicians. Due to the highly nonlinearity of the neural network system, theorems guiding stability and convergence of solutions predicted by the neural network are to be revealed.

Lastly, it would be helpful and interesting if one can theoretically characterize a numerical scheme from the neural network coefficients and learn the forms or mechanics from the scheme and prediction. We leave these questions for further study.

References

- [1] Richard Courant, Kurt Friedrichs, and Hans Lewy. On the partial difference equations of mathematical physics. *IBM journal of Research and Development*, 11(2):215–234, 1967.
- [2] Stanley Osher and James A Sethian. Fronts propagating with curvature-dependent speed: algorithms based on hamilton-jacobi formulations. *Journal of computational physics*, 79(1):12–49, 1988.
- [3] Randall J LeVeque. *Numerical methods for conservation laws*, volume 3. Springer.
- [4] Bernardo Cockburn, George E Karniadakis, and Chi-Wang Shu. *Discontinuous Galerkin methods: theory, computation and applications*, volume 11. Springer Science & Business Media, 2012.
- [5] James William Thomas. *Numerical partial differential equations: finite difference methods*, volume 22. Springer Science & Business Media, 2013.
- [6] Claes Johnson. *Numerical solution of partial differential equations by the finite element method*. Courier Corporation, 2012.
- [7] Grace CY Peng, Mark Alber, Adrian Buganza Tepole, William R Cannon, Suvranu De, Savador Dura-Bernal, Krishna Garikipati, George Karniadakis, William W Lytton, Paris Perdikaris, et al. Multiscale modeling meets machine learning: What can we learn? *Archives of Computational Methods in Engineering*, pages 1–21, 2020.
- [8] Geert Litjens, Thijs Kooi, Babak Ehteshami Bejnordi, Arnaud Arindra Adiyoso Setio, Francesco Ciompi, Mohsen Ghafoorian, Jeroen AWM Van Der Laak, Bram Van Ginneken, and Clara I Sánchez. A survey on deep learning in medical image analysis. *Medical image analysis*, 42:60–88, 2017.
- [9] Jacob Devlin, Ming-Wei Chang, Kenton Lee, and Kristina Toutanova. Bert: Pre-training of deep bidirectional transformers for language understanding. *arXiv preprint arXiv:1810.04805*, 2018.
- [10] Yann LeCun, Léon Bottou, Yoshua Bengio, and Patrick Haffner. Gradient-based learning applied to document recognition. *Proceedings of the IEEE*, 86(11):2278–2324, 1998.
- [11] Alex Krizhevsky, Ilya Sutskever, and Geoffrey E Hinton. Imagenet classification with deep convolutional neural networks. In *Advances in neural information processing systems*, pages 1097–1105, 2012.

- [12] Geoffrey Hinton, Li Deng, Dong Yu, George E Dahl, Abdel-rahman Mohamed, Navdeep Jaitly, Andrew Senior, Vincent Vanhoucke, Patrick Nguyen, Tara N Sainath, et al. Deep neural networks for acoustic modeling in speech recognition: The shared views of four research groups. *IEEE Signal processing magazine*, 29(6):82–97, 2012.
- [13] Jiequn Han, Arnulf Jentzen, and E Weinan. Solving high-dimensional partial differential equations using deep learning. *Proceedings of the National Academy of Sciences*, 115:8505 – 8510, 2018.
- [14] Zichao Long, Yiping Lu, Xianzhong Ma, and Bin Dong. Pde-net: Learning pdes from data. In *International Conference on Machine Learning*, pages 3208–3216, 2018.
- [15] Justin Sirignano and Konstantinos Spiliopoulos. Dgm: A deep learning algorithm for solving partial differential equations. *Journal of computational physics*, 375:1339–1364, 2018.
- [16] Maziar Raissi, Paris Perdikaris, and George E Karniadakis. Physics-informed neural networks: A deep learning framework for solving forward and inverse problems involving nonlinear partial differential equations. *Journal of Computational Physics*, 378:686–707, 2019.
- [17] Uri M Ascher, Steven J Ruuth, and Raymond J Spiteri. Implicit-explicit runge-kutta methods for time-dependent partial differential equations. *Applied Numerical Mathematics*, 25(2-3):151–167, 1997.
- [18] Alex Sherstinsky. Fundamentals of recurrent neural network (rnn) and long short-term memory (lstm) network. *Physica D: Nonlinear Phenomena*, 404:132306, 2020.
- [19] Ricky TQ Chen, Yulia Rubanova, Jesse Bettencourt, and David K Duvenaud. Neural ordinary differential equations. In *Advances in neural information processing systems*, pages 6571–6583, 2018.
- [20] Zhiheng Huang, Wei Xu, and Kai Yu. Bidirectional lstm-crf models for sequence tagging. *arXiv preprint arXiv:1508.01991*, 2015.
- [21] Mike Schuster and Kuldip K Paliwal. Bidirectional recurrent neural networks. *IEEE transactions on Signal Processing*, 45(11):2673–2681, 1997.
- [22] Sepp Hochreiter and Jürgen Schmidhuber. Long short-term memory. *Neural computation*, 9(8):1735–1780, 1997.
- [23] Zachary C Lipton, John Berkowitz, and Charles Elkan. A critical review of recurrent neural networks for sequence learning. *arXiv preprint arXiv:1506.00019*, 2015.
- [24] Alex Graves and Jürgen Schmidhuber. Framewise phoneme classification with bidirectional lstm and other neural network architectures. *Neural networks*, 18(5-6):602–610, 2005.
- [25] Yiping Lu, Aoxiao Zhong, Quanzheng Li, and Bin Dong. Beyond finite layer neural networks: Bridging deep architectures and numerical differential equations. In *International Conference on Machine Learning*, pages 3276–3285, 2018.
- [26] Tomáš Mikolov, Stefan Kombrink, Lukáš Burget, Jan Černocký, and Sanjeev Khudanpur. Extensions of recurrent neural network language model. In *2011 IEEE international conference on acoustics, speech and signal processing (ICASSP)*, pages 5528–5531. IEEE, 2011.
- [27] Kurt Hornik, Maxwell Stinchcombe, Halbert White, et al. Multilayer feedforward networks are universal approximators. *Neural networks*, 2(5):359–366, 1989.
- [28] Fischer Black and Myron Scholes. The pricing of options and corporate liabilities. *Journal of political economy*, 81(3):637–654, 1973.
- [29] Johannes Forster. Mathematical modeling of complex fluids. *Master’s, University of Wurzburg*, 2013.
- [30] Yunkyong Hyon, Chun Liu, et al. Energetic variational approach in complex fluids: maximum dissipation principle. *Discrete & Continuous Dynamical Systems-A*, 26(4):1291, 2010.

- [31] John W Cahn and John E Hilliard. Free energy of a nonuniform system. i. interfacial free energy. *The Journal of chemical physics*, 28(2):258–267, 1958.
- [32] Jean-Luc Guermond, Peter Mineev, and Jie Shen. An overview of projection methods for incompressible flows. *Computer methods in applied mechanics and engineering*, 195(44-47):6011–6045, 2006.
- [33] F. Hecht. New development in freefem++. *J. Numer. Math.*, 20(3-4):251–265, 2012.